PASSIVE ACOUSTIC MONITORING USING RANDOM MATRIX THEORY

Ravi Menon, Peter Gerstoft and William S. Hodgkiss

Marine Physical Laboratory, Scripps Institution of Oceanography
University of California San Diego, La Jolla, CA 92093

ABSTRACT

Cross-correlating ocean noise is a potential alternative to using active sources to monitor and study ocean environments. However, directional sources in the medium (usually ships) often introduce a bias in the cross-correlations, making the travel time estimates unreliable. Here, we use recent results in random matrix theory for the eigenvalue density of isotropic noise sample covariance matrices to separate the directional noise from the diffuse noise field. The eigenvalues obtained from ocean data agree well with the theoretical results. Beamforming on the diffuse noise components reveals a fairly spatially isotropic nature for the noise field, which fits the assumption. The cross-correlations using the diffuse noise field alone converge to the expected travel times (i.e., unbiased estimates) and are stable temporally.

Index Terms— Passive acoustics, environment monitoring, isotropic noise, sample covariance matrix, eigenvalue density

1. INTRODUCTION

In recent years, it has been demonstrated that cross-correlations of noise fields in the environment can be used to obtain travel time and multi-path information [1–5]. It also is possible to image remote areas of the ocean [6, 7] and the interior of the earth [8, 9] using diffuse noise fields, as opposed to using controlled active sources which are both expensive and limited in resolution.

The ocean noise field has two primary components — a rich and varied background diffuse noise field due to wind, breaking waves, biological activities, distant shipping, etc., and a highly directional (and often stronger) noise field due to ships and other similar anthropogenic activities in the vicinity of the observing sensors. Depending on whether one wishes to monitor the changes in the environment, or the movement of the sources, the two components of the noise field can either be beneficial or a deterrant and one of the primary challenges in working with ocean noise is to reliably separate these.

For an N element linear hydrophone array, the sample covariance matrix (SCM) is formed in the frequency domain from M snapshot vectors (i.e., the Fourier coefficients of the data observation vector at a particular frequency f), $\mathbf{x}_m(f),\ m = 1, \ldots, M$ as

$$\widehat{\mathbf{R}}(f) = \frac{1}{M} \sum_{m=1}^{M} \mathbf{x}_m(f)\, \mathbf{x}_m^H(f). \tag{1}$$

The eigendecomposition of $\widehat{\mathbf{R}}(f)$ gives the eigenvalues $\hat{\lambda}_1(f) \geq \cdots \geq \hat{\lambda}_N(f)$ and eigenvectors $\hat{\mathbf{v}}_1(f), \ldots, \hat{\mathbf{v}}_N(f)$. Henceforth, the dependence on f is dropped unless necessary. The objective here is to use statistical inference on the eigenvalues of the SCM from ocean acoustic data, based on theoretical results from random matrix theory (RMT) to separate the two components of the noise field. Random matrix theory has applications in diverse fields, including several in signal processing [10–14]

1.1. Statistical model for the sample covariance matrix

The mth snapshot vector, $\mathbf{x}_m$, is modeled as

$$\mathbf{x}_m = \mathbf{s}_m + \mathbf{n}_m \tag{2}$$

where $\mathbf{s}_m \sim \mathcal{CN}(\mathbf{0}, \mathbf{S})$ is the directional noise vector from loud sources in the environment with a covariance matrix (CM) $\mathbf{S}$ and $\mathbf{n}_m \sim \mathcal{CN}(\mathbf{0}, \mathbf{\Sigma})$ is the N-dimensional Gaussian diffuse noise vector with a CM $\mathbf{\Sigma}$. From the independence of $\mathbf{s}_m$ and $\mathbf{n}_m$, the true covariance matrix of $\mathbf{x}_m$ can be decomposed as

$$\mathbf{R} = \mathbf{S} + \mathbf{\Sigma} \tag{3}$$

To model the effect of a few loud and directional signals, we assume that the rank of $\mathbf{S}$, say K, is small compared to the rank of $\mathbf{\Sigma}$, i.e. $K \ll \mathrm{rank}(\mathbf{\Sigma})$, and that the K non-zero eigenvalues of $\mathbf{S}$ are all larger than the eigenvalues of $\mathbf{\Sigma}$ and manifest in the K largest eigenvalues of the SCM.

The objective is to separate the components of the SCM $\widehat{\mathbf{R}}$ from its eigenvalues and eigenvectors as

$$\begin{aligned} \widehat{\mathbf{R}} &= \sum_{k=1}^{K} \hat{\lambda}_k\, \hat{\mathbf{v}}_k\, \hat{\mathbf{v}}_k^H + \sum_{k=K+1}^{N} \hat{\lambda}_k\, \hat{\mathbf{v}}_k\, \hat{\mathbf{v}}_k^H \\ &= \widehat{\mathbf{R}}_{\mathrm{dir}} + \widehat{\mathbf{R}}_{\mathrm{dif}} \end{aligned} \tag{4}$$

where $\widehat{\mathbf{R}}_{\mathrm{dir}}$ is the directional noise component and $\widehat{\mathbf{R}}_{\mathrm{dif}}$ is the diffuse noise component. The eigenvalues of $\widehat{\mathbf{R}}_{\mathrm{dir}}$, namely $\hat{\lambda}_1, \ldots, \hat{\lambda}_K$ (and the eigenvectors), also contain a diffuse noise component in addition to the directional noise component and hence the separation of $\widehat{\mathbf{R}}$ exactly into $\widehat{\mathbf{S}}$ and $\widehat{\mathbf{\Sigma}}$ is not possible. In order to do so, we first present results from random matrix theory that describe the behavior of the eigenvalues of the SCM when $\widehat{\mathbf{R}} = \widehat{\mathbf{R}}_{\mathrm{dif}} = \widehat{\mathbf{\Sigma}}$, assuming the true noise CM $\mathbf{\Sigma}$ to be spatially isotropic.

2. SPATIALLY ISOTROPIC NOISE FIELDS

The coherence function [15] of the noise recorded on two sensors in a 3D isotropic noise field is $\Gamma = \mathrm{sinc}(2\beta)$, where $\mathrm{sinc}(x) = \sin(\pi x)/(\pi x)$ and β is the ratio of the spacing between the sensors to the wavelength under consideration ($\beta = f\Delta x/c$, where f is the frequency, Δx is the spacing between the sensors, and c is the speed of wave propagation in the medium).

This work was supported by the Office of Naval Research, Grant Nos. N00014-11-1-0321 and N00014-11-1-0320.

2.1. Asymptotic eigenvalues of the isotropic noise CM

For a linear array of N equidistant sensors, the elements of the covariance matrix (CM) of the noise field (normalized to unit power on each sensor) are given by $\mathbf{\Sigma}_{ij} = \operatorname{sinc}(2\beta|i-j|)$, which is a symmetric Toeplitz matrix. Thus, the spatial correlations are only dependent on β (or equivalently, on f) and the separation $|i-j|$.

It was shown in [14] that there are at most two distinct eigenvalues (with multiplicities) for all β, given by

$$\Lambda_1 = \frac{q+1}{2\beta} \text{ and } \Lambda_2 = \frac{q}{2\beta}, \tag{5}$$

with $q \in \{0, 1, \dots\}$ such that $q < 2\beta \leq q+1$, and the respective multiplicity ratios are given by

$$\xi_1 = 2\beta - q \text{ and } \xi_2 = q + 1 - 2\beta. \tag{6}$$

A key result here is the fact that the CM is rank deficient for $\beta < 1/2$, because $\Lambda_2 = 0$, i.e. the rank deficiency is inherent and not as a result of snapshot deficiency.

2.2. Eigenvalue density of the isotropic noise SCM

The isotropic noise SCM $\widehat{\mathbf{\Sigma}}$ is modeled as

$$\widehat{\mathbf{\Sigma}} = \frac{1}{M} \mathbf{\Sigma}\, \mathbf{X}\mathbf{X}^H \tag{7}$$

where $\mathbf{X}$ is an $N \times M$ random matrix whose entries are zero-mean complex Gaussian random variables drawn from $\mathcal{CN}(0,1)$. The probability density of the eigenvalues of the noise SCM were derived in [14] in the limit $N, M \to \infty,\ N/M \to \nu$, using Stieltjes transforms [16]. Here, we only consider $\nu \leq 1$, i.e. there are more number of snapshots than the number of hydrophones.

When the ratio of spacing to wavelength $\beta < 1/2$ or is a multiple of $1/2$ i.e., $\beta = q/2,\ q \in \mathbb{N}$, the eigenvalue density is given by,

$$\widehat{\mathrm{p}}(\lambda) = \begin{cases} \xi_1 \frac{\sqrt{(\lambda_+ - \lambda)(\lambda - \lambda_-)}}{2\pi\nu\lambda} + \xi_2 \delta(\lambda) & \lambda_- < \lambda < \lambda_+ \\ \text{otherwise} \end{cases} \tag{8}$$

where

$$\lambda_\pm = \left(\sqrt{\Lambda_1} \pm \sqrt{\nu}\right)^2 \tag{9}$$

Regardless of the value of ν, $\widehat{\mathbf{\Sigma}}$ will be rank deficient for all $\beta < 1/2$, as $\xi_2 \neq 0$.

For all other values of β, the eigenvalue density of the SCM is given by,

$$\widehat{\mathrm{p}}(\lambda) = \frac{1}{\pi} \left| \operatorname{Im}\left[\frac{\left(1 + \imath\sqrt{3}\right) R}{2} + \frac{\left(1 - \imath\sqrt{3}\right) Q}{2R} \right] \right|, \tag{10}$$

where $R = \sqrt[3]{P + \sqrt{-D}}$, $Q = (a_2^3 - 3a_1)/9$, $D = Q^3 - P^2$ and $P = (-2a_2^3 + 9a_1a_2 - 27a_0)/54$ and a_i being the coefficients of x in the polynomial

$$\begin{aligned} &x^3\lambda^2\Lambda_1\Lambda_2\nu^2 + x^2\lambda\nu\left[\lambda(\Lambda_1+\Lambda_2) + 2\Lambda_1\Lambda_2(\nu-1)\right] \\ &+ x\left[\lambda^2 + \lambda\nu(\Lambda_2\xi_1 + \Lambda_1\xi_2) + \lambda(\Lambda_1+\Lambda_2)(\nu-1)\right. \\ &\left.+\Lambda_1\Lambda_2(\nu-1)^2\right] + \lambda + (\Lambda_1\xi_2 + \Lambda_2\xi_1)(\nu-1) = 0. \end{aligned} \tag{11}$$

when it is written in the form $x^3 + a_2x^2 + a_1x + a_0$. The dependence on β in both Eq. (8) and Eq. (10) arises from the definitions of Λ_i and ξ_i from Eq. (5) and Eq. (6) respectively.

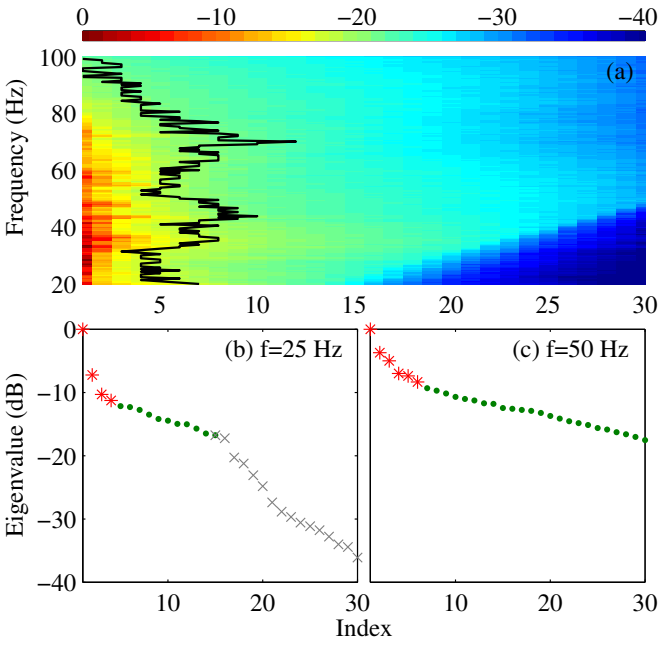

Fig. 1. (a) Eigenvalues of the data SCM $\widehat{\mathbf{R}}$ (dB) from 20–100 Hz. The solid line shows the threshold separating the directional noise (to the left) from the diffuse noise. (b, c) Individual eigenvalues at 25 and 50 Hz due to ships ($*$), diffuse noise ($\bullet$) and eigenvalues not considered [$\times$, only in (b)]. The chosen time slices correspond to data time 92 min in Fig. 3.

An important observation is the fact that the eigenvalue densities have a finite support on the real line, i.e., the density is zero outside certain bounds. The asymptotic upper bound for all β and $\nu \leq 1$ can be written as

$$\zeta(\beta, \nu) = \begin{cases} \lambda_+ & \beta < 1/2 \bigvee \beta = q/2,\ q \in \mathbb{N} \\ \lambda'_+ & \text{otherwise} \end{cases} \tag{12}$$

where λ'_+ is the largest root of D (as a function of β and ν).

3. INFERENCE FROM THE EIGENVALUES OF THE SCM

The statistical inference approach followed is based on [17], but using the asymptotic upper bound to threshold the eigenvalues instead of the Tracy–Widom distributions used there. Similar algorithms are also used in signal processing [12] for signal detection. At each β (or frequency f), we test sequentially the eigenvalues $\hat{\lambda}_i$ of $\widehat{\mathbf{R}}$ at each step k (starting with $k = 1$) against the following two hypotheses $\mathcal{H}_0$ (null) and $\mathcal{H}_1$:

$$\begin{aligned} &\mathcal{H}_0 : \textit{The kth eigenvalue is due to diffuse noise} \\ &\mathcal{H}_1 : \textit{The kth eigenvalue is dominated by loud sources} \end{aligned} \tag{13}$$

until $\mathcal{H}_0$ no longer can be rejected.

Since, $\hat{\lambda}_1$ is bounded (asymptotically) by the upper bound of the density (the effect of the tail for finite N is ignored here), i.e.,

$$\frac{\hat{\lambda}_1}{\hat{\sigma}^2(1)} \leq \zeta\left(\beta, \frac{N}{M}\right) \tag{14}$$

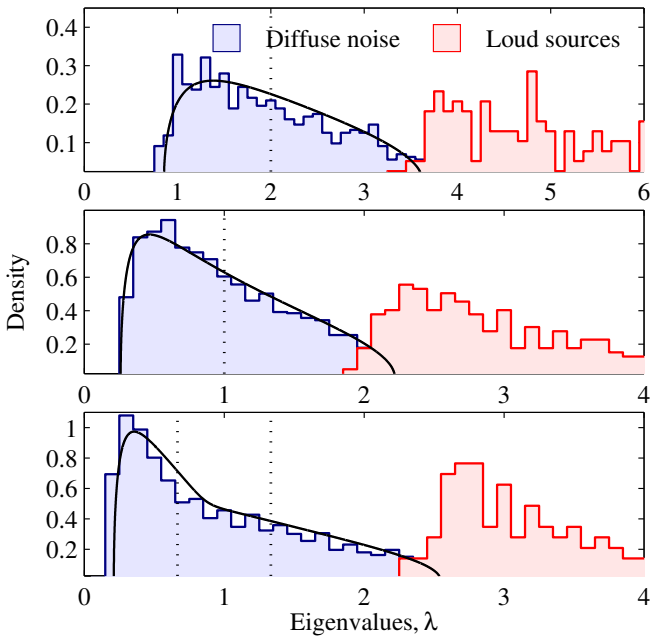

Fig. 2. Empirical eigenvalue density (histogram) of the eigenvalues of $\widehat{\mathbf{R}}_{\text{dif}}$ (under the solid lines) and $\widehat{\mathbf{R}}_{\text{dir}}$ (to the right) obtained from ocean acoustic data for f = (a) 25 Hz, (b) 50 Hz and (c) 75 Hz. The solid lines correspond to the asymptotic eigenvalue density. In (a), only the contribution from the largest $\lfloor \xi_1 N \rfloor$ eigenvalues are shown. The dotted lines show the location of Λ_1, the eigenvalue of the isotropic noise CM. The densities for the eigenvalues of $\widehat{\mathbf{R}}_{\text{dir}}$ extend beyond the extent of the panels and is truncated for clarity.

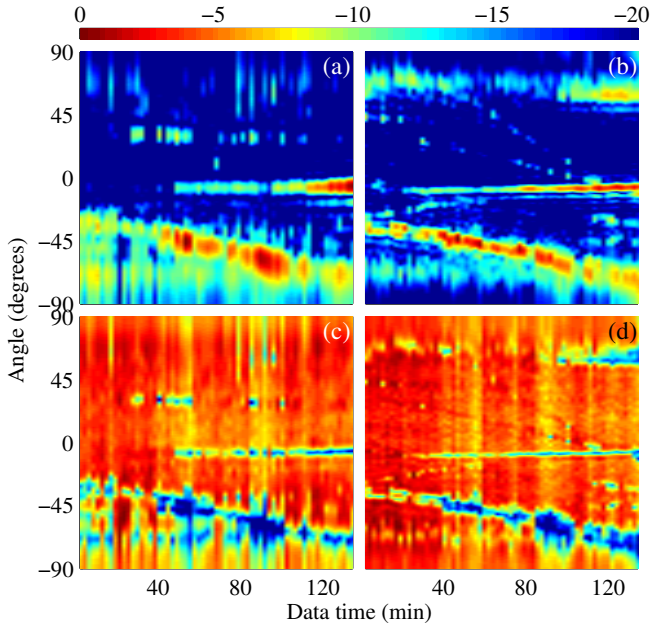

Fig. 3. (a,b) Conventional beamformer output (dB) at 25 and 50 Hz respectively using $\widehat{\mathbf{R}}_{\text{dir}}$. (c,d) Same as the previous, using $\widehat{\mathbf{R}}_{\text{dif}}$. The output in each panel is normalized by the maximum in that panel.

where $\hat{\sigma}^2(k) = (N-k+1)^{-1} \sum_{i=k}^{N} \hat{\lambda}_i$ is a normalization factor to bring the mean of the eigenvalues, or the average power to 1 (this is done to enable comparison with the analytical results which were derived for unit noise power), $\mathcal{H}_0$ is rejected if the inequality is not satisfied.

The routine is then repeated for the remaining $N-1$ eigenvalues, this time testing $\hat{\lambda}_2$, and using $\hat{\sigma}^2(2)$ (i.e., incrementing k), and so on until we fail to reject $\mathcal{H}_0$. The final value of $K' = k-1$ gives the number of eigenvalues that have been *effectively* identified to be due to directional sources.

For $\beta < 1/2$, the smallest $\lfloor \xi_2 N \rfloor$ eigenvalues are theoretically zero. In practice however, they're not *exactly* zero, most likely due to sensor noise. It was observed empirically that including these eigenvalues in the approach resulted in the lhs in (14) often being large, leading to $\mathcal{H}_0$ being rejected with a greater likelihood. To avoid this, an *ad hoc* correction is made by not considering these eigenvalues for $\beta < 1/2$ and subsequently, N is replaced with $N' = \lfloor \xi_2 N \rfloor$ in (14) and $\hat{\sigma}^2(k)$ is redefined as $\hat{\sigma}^2(k) = \Lambda_1 (N'-k+1)^{-1} \sum_{i=k+1}^{N'} \hat{\lambda}_i$ for $\beta < 1/2$.

Using the asymptotic upper bound ζ automatically sets the significance level, α as well, which varies with β. Hence it is not possible to test at a uniform α or a chosen α.

4. EXPERIMENTAL RESULTS

The data considered here were recorded from 13:00:00 to 15:14:24 on September 1, 2006 (UTC) on the first 30 hydrophones of a 32 element bottom mounted horizontal line array (HLA), at a water depth of 79 m with a 15 m inter-element spacing. The experiment was part of the Shallow Water 2006 (SW06) experiments conducted off the coast of New Jersey. The data were filtered to 20–100 Hz and the SCM was formed from 125 snapshots every 128 s (each snapshot lasts 1.024 s).

4.1. Eigen-structure of the ocean noise field

Fig. 1 shows the eigenvalues across all frequencies at a single time slice (128 s from 14:31:44). The threshold obtained from the approach in Section 3 is shown by the solid line. The dark triangle to the lower right is the region with zero eigenvalues (theoretically) and corresponds to invisible space. This is also observed in Fig. 1 (b), where the eigenvalues drop past the 16th eigenvalue, which closely corresponds to $\lfloor \xi_2 N \rfloor$, as predicted by theory (6).

It is clear that the algorithm separates the diffuse noise field from the directional noise field quite well. The histogram of the non-zero eigenvalues of $\widehat{\mathbf{R}}_{\text{dif}}$ (Fig. 2) for the entire duration (normalized to unit mean at each time slice) shows good agreement with the asymptotic density (solid line). The histogram of the eigenvalues of $\widehat{\mathbf{R}}_{\text{dir}}$ lies to the right of the diffuse noise eigenvalues.

4.2. Applicability in passive monitoring

Conventional beamforming with Hamming spatial shading was performed for each block for $\widehat{\mathbf{R}}_{\text{dir}}$ and $\widehat{\mathbf{R}}_{\text{dif}}$ at 25 and 50 Hz as:

$$B_{(\cdot)}(\theta) = \mathbf{w}^H(\theta)\, \widehat{\mathbf{R}}_{(\cdot)}\, \mathbf{w}(\theta), \tag{15}$$

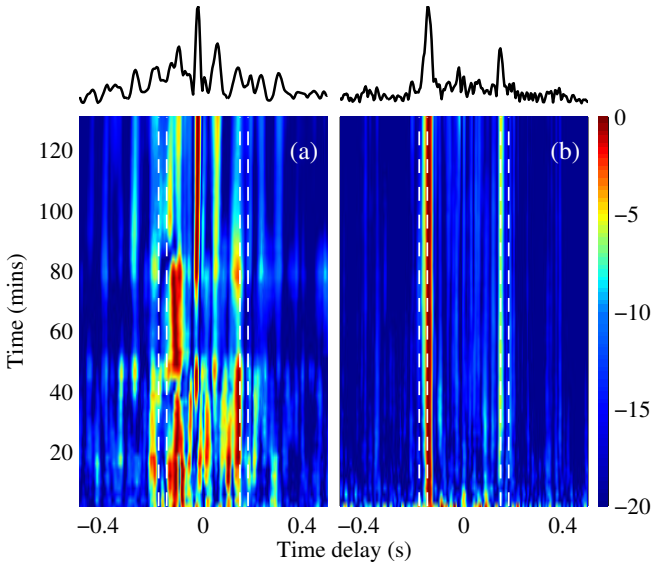

Fig. 4. Averaged cross-correlations (dB) between phones 1 and 16 obtained using (a) $\widehat{\mathbf{R}}$ and (b) $\widehat{\mathbf{R}}_{\rm dif}$ with increasing averaging time. The maximum in each trace has been normalized to 1 for plotting purposes in order to highlight the peaks. The result after averaging or 136.5 min (solid) is shown above the respective plots. Dashed lines indicate the expected travel times for the direct (inner) and the surface reflected (outer) paths.

where $\mathbf{w}(\theta)$ is the shaded steering vector, with the phase delay of the nth element given by $w_n(\theta) = \exp\left[\imath 2\pi f n d/c \, \sin(\theta)\right]$, $n = \{0, 1, \ldots, N-1\}$.

Using $\widehat{\mathbf{R}}_{\rm dir}$, the tracks from loud sources detected by the algorithm are resolved with a high SNR [Fig. 3(a,b)]. Beamforming using $\widehat{\mathbf{R}}_{\rm dif}$ indicates that the diffuse noise field is fairly isotropic, with nulls only at directions where the ships were removed.

The averaged time domain cross-correlation between phones i and j using ocean noise is obtained as

$$\widehat{C}_{ij}(t) = \mathcal{F}^{-1}\left[\left\langle \widehat{\mathbf{R}}_{ij}(f)\right\rangle_T\right] \qquad (16)$$

where t denotes the correlation time, T denotes the averaging time and $\mathcal{F}^{-1}$ denotes an inverse Fourier transform. When the cross-correlations are obtained from $\widehat{\mathbf{R}}$ (averaged cumulatively) [Fig. 4 (a)], the arrival times are skewed by the directional sources seen in Fig. 3 (a,b) and hence are not reliable. On the other hand, obtaining the cross-correlations using $\widehat{\mathbf{R}}_{\rm dif}$ in (16) instead of $\widehat{\mathbf{R}}$ results in a steady estimate of the arrival time that corresponds to the expected travel time [Fig. 4 (b)].

5. CONCLUSIONS

The theoretical distributions for the eigenvalues of an isotropic noise field have been used to study ocean noise. It is demonstrated that using the eigenvalues of the sample covariance matrix, the ocean noise field can be separated into a directional noise component (nearby shipping and other sources) and a diffuse noise component. The directional noise component provides a higher signal-to-noise ratio in beamforming applications, which can be used to detect and observe the sources. Using the diffuse noise component in noise cross-correlations yields stable travel time estimates, which has applications in studying and monitoring environments passively.

6. REFERENCES

[1] R. L. Weaver and O. I. Lobkis, "Ultrasonics without a source: Thermal fluctuation correlations at MHz frequencies," *Phys. Rev. Lett.*, vol. 87, pp. 134301, 2001.

[2] O. I. Lobkis and R. L. Weaver, "On the emergence of the Green's function in the correlations of a diffuse field," *J. Acoust. Soc. Am.*, vol. 110, pp. 3011–3017, December 2001.

[3] P. Roux, W. A. Kuperman, and the NPAL group, "Extracting coherent wave fronts from acoustic ambient noise in the ocean," *J. Acoust. Soc. Am.*, vol. 116, pp. 1995–2003, 2004.

[4] K. G. Sabra, P. Gerstoft, P. Roux, W. A. Kuperman, and M. C. Fehler, "Extracting time-domain Green's function estimates from ambient seismic noise," *Geophys. Res. Lett*, vol. 32, pp. L03310, 2005.

[5] L. A. Brooks and P. Gerstoft, "Green's function approximation from cross-correlations of 20-100 Hz noise during a tropical storm," *J. Acoust. Soc. Am.*, vol. 125, pp. 723–734, Jan 2009.

[6] M. Siderius, C. H. Harrison, and M. B. Porter, "A passive fathometer technique for imaging seabed layering using ambient noise," *J. Acoust. Soc. Am.*, vol. 120, pp. 1315–1323, 2006.

[7] J. Traer, P. Gerstoft, and W. S. Hodgkiss, "Ocean bottom profiling with ambient noise: A model for the passive fathometer," *J. Acoust. Soc. Am.*, vol. 129, no. 4, pp. 1825–1836, 2011.

[8] N. M. Shapiro, M. Campillo, L. Stehly, and M. H. Ritzwoller, "High-resolution surface-wave tomography from ambient seismic noise," *Science*, vol. 307, pp. 1615–1618, 2005.

[9] P. Gerstoft, K. G. Sabra, P. Roux, W. A. Kuperman, and M. C. Fehler, "Green's functions extraction and surface-wave tomography from microseisms in southern California," *Geophysics*, vol. 71, pp. SI23–SI31, 2006.

[10] X. Mestre, "On the asymptotic behaviour of the sample estimates of eigenvalues and eigenvectors of covariance matrices," *IEEE Trans. Signal Proc.*, vol. 56, no. 11, pp. 5353–5368, 2008.

[11] R. R. Nadakuditi and A. Edelman, "Sample eigenvalue based detection of high-dimensional signals in white noise using relatively few samples," *IEEE Trans. Signal Process.*, vol. 56, no. 7, pp. 2625–2638, 2008.

[12] R. R. Nadakuditi and J. W. Silverstein, "Fundamental limit of sample generalized eigenvalue based detection of signals in noise using relatively few signal-bearing and noise-only samples," *IEEE Journal of selected topics in Signal Processing*, vol. 4, no. 3, pp. 468–480, 2010.

[13] J. R. Buck and K. Wage, "Modeling dominant mode rejection beamformer notch depth using random matrix theory," 162nd meeting of the Acoust. Soc. Am., San Diego, CA, USA (November 2011).

[14] R. Menon, P. Gerstoft, and W. S. Hodgkiss, "Asymptotic eigenvalue density of noise covariance matrices," *IEEE Trans. Signal Proc.*, 2012, DOI: 10.1109/TSP.2012.2193573.

[15] H. Cox, "Spatial correlation in arbitrary noise fields with application to ambient sea noise," *J. Acoust. Soc. Am.*, vol. 54, no. 5, pp. 1289–1301, 1973.

[16] J. W. Silverstein, "Strong convergence of the empirical distribution of eigenvalues of large dimensional random matrices," *J. Multivar. Anal.*, vol. 54, pp. 175–192, 1995.

[17] I. M. Johnstone, "On the distribution of the largest eigenvalue in principal components analysis," *Ann. Statist.*, vol. 29, no. 2, pp. 295–327, 2001.